nature reviews physics

https://doi.org/10.1038/s42254-026-00981-2

Review article

Check for updates

Interplay of topology and reversible associations in multi-responsive macromolecular networks

Evelyne van Ruymbeke[1] & Dimitris Vlassopoulos[2,3]

Abstract

Macromolecular networks have been central to the evolution of polymers as versatile materials with applications from the chemical and pharmaceutical industry to packaging and biotechnology. The main scientific challenge is to develop design criteria for fabricating networks with desired performance. To this end, it is crucial to relate the molecular behaviour of components to the macroscopic properties of the network. At the same time, the advances in macromolecular chemistry offer molecular insights that enhance our ability to tailor their properties, for example, by combining reversible bonds with macromolecular architecture. To meet the ambitious goal of molecular design, it is important to organize the current knowledge, understand the key physical concepts governing the response of different classes of networks and unify the underlying principles, as well as open challenges and perspectives. Here we focus on the rheology of networks based on physical (reversible) associations, in the melt state, and offer a concise view of the state-of-the-art along with the current directions and perspectives in this field.

Sections

Introduction

Mesh size and related rubbery plateau in transient polymer networks

Networks based solely on entanglements

Networks based on dynamic intermolecular bonding

Nonlinear viscoelasticity of complex macromolecules and transient networks

Dual and double networks combining two types of associations

Outlook

[1]Bio- and Soft Matter, Institute of Condensed Matter and Nanosciences, Université catholique de Louvain, Louvain-la-Neuve, Belgium. [2]Department of Materials Science and Engineering, University of Crete, Crete, Greece. [3]Institute of Electronic Structure and Laser, FORTH, Crete, Greece. e-mail: evelyne.vanruymbeke@uclouvain.be; dvlasso@iesl.forth.gr

Key points

- Long linear, star and more complex branched polymers form (transient) entanglement networks, exhibiting strain softening and hardening in start-up shear and elongation, respectively. They flow at steady state, characterized by shear thinning and elongational thinning at high strain rates.

- Transient networks based on unentangled building blocks offer a large tunability in elastic modulus and relaxation times. Under large nonlinear deformation, their maximum stretchability is limited to the mesh size of the network, and brittle fracture is often observed.

- Combining transient junctions and entanglements in a polymer network allows keeping a relatively small mesh size, while preserving a good extensibility that is governed by the transient junctions.

- Branching and sticky junctions along a polymeric chain act as additional friction, delaying its relaxation time. Conversely, long chain branching promotes dynamic dilution of an entanglement network, facilitating its flow.

Introduction

Polymeric and elastomeric networks are ubiquitous in nature and applications and, at the same time, offer many challenges in polymer and soft material physics. In the years since early work on modelling rubber elasticity[1–3], important advances have been made and the range of network applications keeps on expanding[4–6]. However, changing socio-economic conditions and the urgent need to address environmental concerns arising from the excessive use of plastics and elastomers call for the development of new functional networks with enhanced versatility[7].

For polymers to be useful, their rheological properties in the bulk (melt) state — characterized by quantities such as the viscosity and the storage modulus — must fall within the window required for the desired application. It is therefore valuable to understand and develop methods for linking polymer conformation and composition to the rheology. In this regard, the coupling of macromolecular parameters with different types of associations seems to be the way forward.

In physical polymer networks — the focus of this Review — the transient connectivity arises from two principal mechanisms: topological entanglements and reversible supramolecular associations. In the former, entanglements play the role of temporary crosslinking junctions. Classical reptation theory explains how entanglements restrict motion in linear systems[4,6,8]. This framework has been extended to branched polymers, where it predicts hierarchical relaxation starting from the outer dangling ends and proceeding inward via arm retraction and constraint release[9,10]. However, our ability to tailor the properties of entangled polymers is limited: for most polymers the entanglement plateau modulus varies over a relatively small range of 10^5–10^6 Pa.

To enlarge the window of processability and applications, more complex polymer architectures (or composition), including covalent or reversible junctions are of interest, as they offer many ways to modulate the dynamics of the networks obtained. They can be understood in terms of the sticky Rouse and sticky reptation frameworks, in which the stickers generate time-dependent constraints whose lifetime governs viscoelastic behaviour[11,12]. A systematic comparison of the impact of frictional resistance due to topology (macromolecular architecture) or chemistry (associating groups) paves the way to tailor network strength and relaxation dynamics at molecular scale, both in linear and nonlinear rheology. Therefore, there have been many investigations[13–28] of how the formation and properties of networks are influenced by the interplay of entropic (chain elasticity) and enthalpic (associations, copolymerization) effects with polymer architecture and by the presence of topological constraints (such as entanglements or loop threading) and reversible associations (for example ionic or hydrogen bonding or metal–ligand interactions). These factors translate into seven control parameters, related to the chain (flexibility, molar mass and architecture) and to the reversible junctions (nature, density, strength and location).

In this Review, we first discuss the viscoelastic properties of physical networks made solely from entanglements. We then show how these properties can be tuned if the macromolecules contain a few chemical crosslinking junctions, to create complex architectures (for example stars, combs or dendritic Cayley trees). The main effect of chain branching is to act as a source of additional friction, slowing down the relaxation dynamics and enhancing strain hardening under uniaxial extension. Here we discuss only uniaxial extension that we call simply extension or elongation. To assess physical networks based on branched polymers and physically associating polymers, it is necessary to critically compare them. In the linear viscoelastic regime the terminal relaxation of both types of networks slows down, being controlled either by the dynamics of the branching chains or by the dynamics of the reversible associations (sticky junctions), but large differences may appear under large deformation. Subsequently, guided by this comparison, we discuss the effects of topological entanglements versus sticky junctions on the network properties. Although they both lead to a similar decrease of the mesh size of the polymer network, entanglement dynamics is governed by chain sliding, which is not the case for sticky junctions, and this has large consequence on the network extensibility. Further, we briefly address the properties of other types of physical networks (slide ring gels, rings, associating networks based on phase separation and dual networks with two different types of sticky groups).

The punchline is the emerging ability to tailor the rheology of such networks at molecular scale and to design networks with desired response. The existence of more than one control parameter (entanglements, macromolecular architecture, stickers with different strength and enthalpic interactions) makes this broad class of networks multi-responsive.

Our discussion links molecular parameters (controlled by chemistry) with macroscopic properties (controlled by rheology). The pertinent molecular parameters are listed in Fig. 1a. In addition, there are important external or environmental parameters such as temperature, pressure, humidity and load (for example, deformation or stress); here, we address the role of the latter only[29,30].

Mesh size and related rubbery plateau in transient polymer networks

The rubbery plateau refers to the region in the relaxation spectrum of a polymer network at intermediate time scales, in which the storage modulus G' is approximately constant with a value G_N^0. In chemical networks the rubbery plateau arises from the permanent crosslinks (Fig. 1b), whereas in polymer melts the (transient) rubbery plateau arises from topological constraints — the interchain entanglements that restrict the renewal of chain conformation at the entanglement length scale, which corresponds to the average distance between these constraints and defines the mesh size of the entanglement network

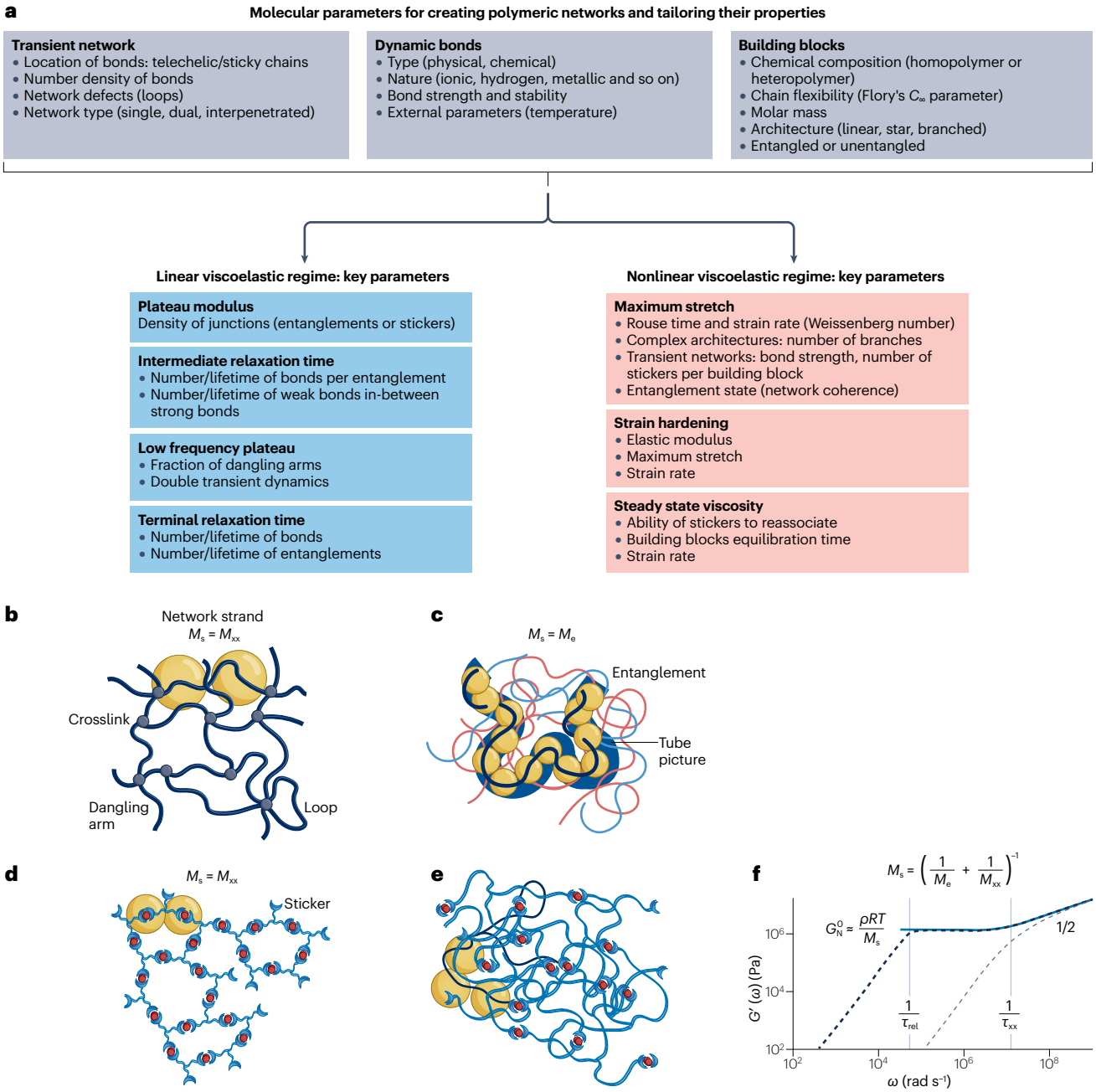


Fig. 1 | Overview of this Review. Parameters considered in this Review (panel **a**). Polymeric networks based on chemical crosslinks: the molar mass of the mesh size M_s is equal to M_{xx}, the average molar mass between two crosslinks (panel **b**), topological entanglements. M_s is equal to M_e, the average molar mass between two entanglements (panel **c**) and physical crosslinks with unentangled (panel **d**) or entangled (panel **e**) strands in between. The blobs and the tube picture, junctions, dangling ends, network strands and loops are also shown. **f**, Representation of the frequency (ω)-dependent storage modulus G': contrary to the response of unentangled and non-sticky building blocks (thin dashed curve to the left), a rubbery plateau is observed for chemical and physical polymer networks, starting at the equilibration time of a network strand, τ_{xx}. Physical networks flow at long relaxation time (τ_{rel}) (thicker dashed curve), whereas chemical networks do not relax (continuous blue curve).

(Fig. 1c). Therefore, the rubbery plateau is determined by the density of topological constraints and is commonly expressed as an ideal network[6]

$$G_N^0 = \frac{\rho RT}{M_e} = G_{N,ent}^0, \quad (1)$$

in which M_e is the entanglement molar mass, ρ is the density, R the gas constant and T the temperature. In the linear viscoelastic regime, the elasticity arises purely from topological confinement, and chain relaxation proceeds at long time scales, at which the chains can diffuse on a length scale corresponding to their size.

In associating polymer networks, the constraints are due to reversible bonding between chains, which represents transient crosslinking points. For unentangled chains with sufficiently large density of bonding motifs (stickers) to form a network (Fig. 1d), the effective modulus is governed by these transient bonds

$$G_N^0 = \frac{\rho RT}{M_{xx}} = G_{N,xx}^0, \quad (2)$$

in which M_{xx} is the average molar mass between two reversible junctions. Its relaxation depends on the lifetime of active junctions and on the composition of the building blocks.

If the transient network combines entanglements and reversible junctions (Fig. 1e), both types of constraints contribute to the rubbery plateau[6]

$$\frac{1}{M_s} = \frac{1}{M_e} + \frac{1}{M_{xx}} \quad (3)$$

$$G_N^0 = \frac{\rho RT}{M_s} = \frac{\rho RT}{M_e} + \frac{\rho RT}{M_{xx}} = G_{N,ent}^0 + G_{N,xx}^0, \quad (4)$$

in which M_s is the average molar mass between two physical constraints.

Polymer networks often include dangling arms — segments connected to the network via a single junction — which are not trapped in the network (Fig. 1b). In associating polymers, these arise from building block architectures with no terminal functional groups. The presence of dangling arms effectively reduces the number of elastically active strands and thus lowers the value of the rubbery plateau[6,9]. When dangling arms are long enough to be entangled, they may initially contribute to the entanglement plateau, but ultimately, they relax on time scales governed by arm retraction. Moreover, the possible fluctuations of network junctions effectively soften the network, something not accounted for in the ideal network model. This effect is included in the phantom network model that is appropriate for lightly crosslinked systems[6,30]

$$G_{N,xx}^0 = \frac{\rho RT}{M_{xx}}\left(1 - \frac{2}{f}\right), \quad (5)$$

in which f is the functionality of the junction (the nominal number of chain segments linked to a junction).

In this Review, we discuss how the interplay of lifetimes of entanglements, reversible crosslinks and branch relaxation dictates the rheological properties of physical networks. To this end, we compare conventional branched and associating linear polymers. This conceptual framework links molecular architecture, thermodynamics (for example, possible clustering or microphase separation of the stickers) and network dynamics, opening the route to rationally design transient polymer networks with tailored rubbery elasticity and dissipation profile.

Networks based solely on entanglements

Linear or star building blocks

In the linear regime of deformation, at short times the topological entanglements act as physical crosslinks, preventing the chains from relaxing and renewing their configuration. The environment where they can freely move is described by a tube that surrounds the chain's contour[4–6] (Fig. 1c). For linear polymers, the main relaxation process is reptation, which describes how a chain escapes from its tube through a thermally activated curvilinear diffusion process along its own contour (Fig. 2a). This process is possible because of the ability of the two free ends to randomize their direction and enable the forward and backward diffusion, which eventually leads to loss of memory of the initial tube, in other words, chain relaxation. The longer the chain is, the longer is the distance that the chain must cover to escape the tube and the larger the chain friction. Therefore, the corresponding relaxation time strongly depends on the molar mass[4]. Although it should scale as $\tau_{rept} \propto M^3$, a slightly higher exponent is found experimentally ($\tau_{rept} \propto M^{3.4}$) due to the fast fluctuations of the chain extremities, which speed up the reptation (this process is called contour length fluctuations, CLF). There is an additional process, thermal constraint release, that is particularly important in polydisperse linear polymers or branched polymers[4–6,31] and is briefly described below.

Star polymers display qualitatively different viscoelastic signatures to those of linear polymers. They are unable to reptate due to the presence of the branching point (core), that acts as an effective stagnation point. Consequently, each arm retracts along its own contour via fluctuations to release its initial entanglements and renew its configuration[9,10,32]. This process is entropically unfavourable, and the corresponding relaxation time corresponds to the motion of the free end against a quadratic potential on the molecular segment depth, x, that ranges from $x = 0$ at the arm extremity to $x = 1$ at the branching point, $\tau_{fluc} \propto \exp(M_{arm}x^2)$. This process leads to the broad terminal relaxation (and loss modulus) of the star arms, whereas the storage modulus decreases logarithmically with decreasing angular frequency of oscillatory deformation[32] (Fig. 2b).

Despite their large difference in the linear regime, the nonlinear elongational properties of linear and star polymer melts are very similar, because the time needed for a stretched chain to return to its equilibrium (coil) configuration (the Rouse time, τ_R) is similar[33,34]. The extensional deformation is described by the Hencky strain $\varepsilon = -2\ln(\frac{d}{d_0})$, in which d is the diameter of a deformed cylindrical filament of original diameter d_0. For large Hencky strain rate $\dot{\varepsilon}$ such that the Rouse Weissenberg number $Wi_R = \dot{\varepsilon}\tau_R$ is larger than 1, the chains do not have time to equilibrate their monomeric tension along their whole backbone and they stretch[34,35]. This stretching leads to transient strain hardening (increase of transient extensional viscosity with time at a given imposed extensional rate) (Fig. 2c). Nevertheless, because entanglements are not fixed constraining points, chains can slide through these entanglements, and monomeric tension equilibration is not limited within a single entanglement segment. This sliding process reduces the maximum stretch the chains can reach, leading to extension thinning in the steady-state regime, in which the entangled network is unable to resist on longer time scales[36–38]. Note that the equilibration time of a chain in the nonlinear regime is not equal but proportional to τ_R and is affected by the chemical nature of the molecules[39,40]. Moreover, the importance of the transient hardening depends on the entanglement state of the chains when they start to stretch, the latter state depending on the sample's molecular characteristics (such as its polydispersity)[41,42].

Under nonlinear shear flow, the steady-state viscosity exhibits shear thinning. In general, the thinning slope depends on the state of entanglement and typically covers the range from −0.5 to −0.9 (refs. 5,43–45). The transient response is characterized by strain softening, which becomes more pronounced on increasing the shear rate. An overshoot in the transient shear stress is commonly associated with the occurrence of conformational rearrangements (orientation and stretch) before steady-state flow is established (Fig. 2d). The decrease of transient stress from overshoot to steady state reflects chain reorientation and partial release of entanglements[46].

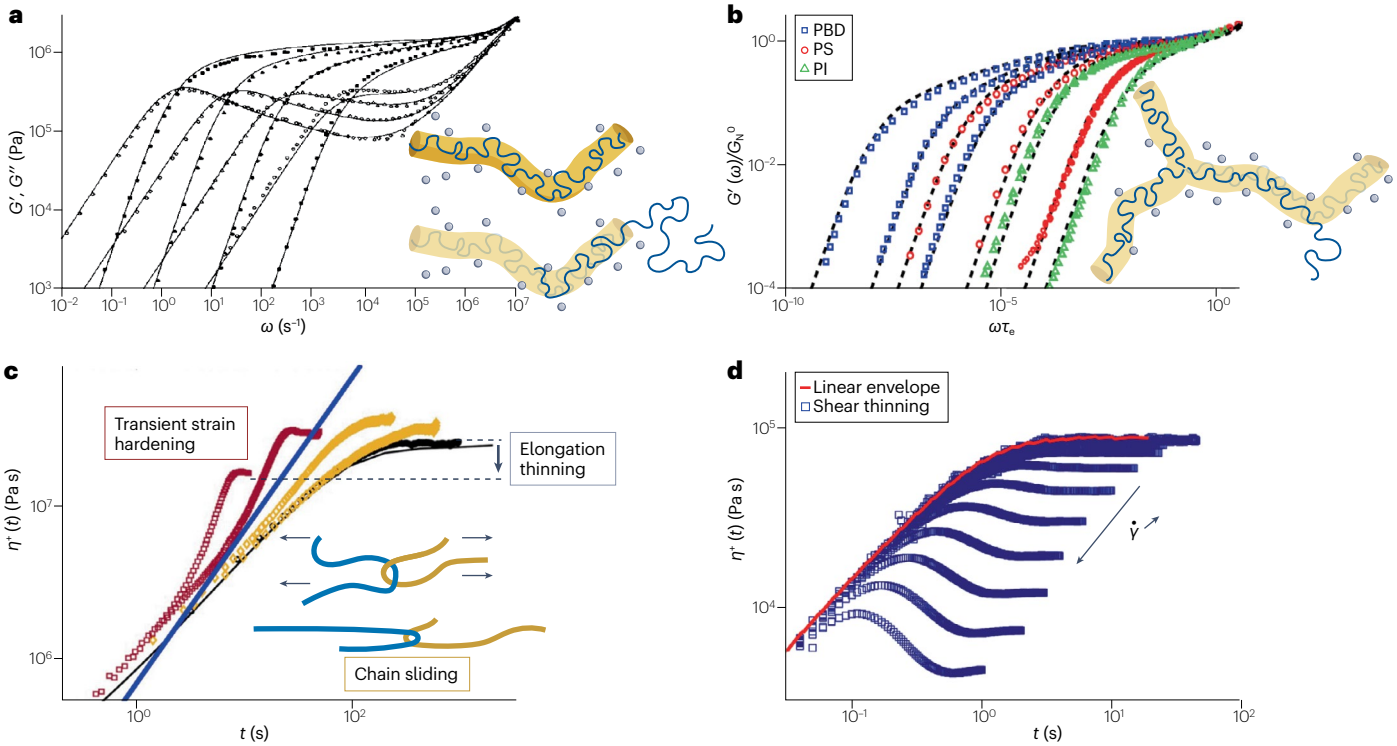


Fig. 2 | Rheological signatures of entangled linear and star polymers. **a**, Storage and loss moduli (G' and G'') as a function of the frequency ω for linear polybutadiene (PBD) melts (1,4-addition) of increasing molar mass (from right to the left: M = 20.7, 44.1, 97 and 201 kg mol^{-1}). The inset shows illustration of the tube escape mechanism. **b**, Normalized frequency dependent storage modulus of star 1,4-polyisoprene (PI), polystyrene (PS) and polybutadiene melts containing (from right to left) and increasing number of entanglements per arm. The logarithmic decay of G' and broad relaxation of G'' are evident. The inset shows the tube escape. **c**, Transient viscosity (stress growth coefficient) η^+ in uniaxial extension (extensional stress growth coefficient) as a function of extension time t for linear polystyrene with a molar mass of 100 kg mol^{-1} at different stretch rates (increasing from right to left). The inset shows a mechanism of elongation of linear chains. **d**, Transient viscosity in shear (shear stress growth coefficient) for linear polystyrene with a molar mass of 133 kg mol^{-1} at different shear rates $\dot{\gamma}$ (increasing from top to bottom). Panel **a** adapted with permission from ref. 146, ACS and ref. 147, Springer Nature Limited. Panel **b** adapted with permision from ref. 148, ACS. Panel **c** adapted with permission from ref. 149, AIP. Panel **d** adapted with permission from ref. 150, ACS.

Complex architectures and hierarchical relaxation

Further branching can be achieved with complex macromolecules that typically consist of a backbone and several branches. Some examples, with increasing complexity, include H-polymer (linear backbone with two branches attached to each end), pompom (such as H-polymer but with many branches at the ends), (linear) comb (with different branches along a linear backbone), star-comb (same as linear comb but with star polymer backbone) and Cayley trees (dendritically branched polymers)[47–51]. In the example of comb polymers (Fig. 3a), their relaxation takes place hierarchically: first, their branches relax by retraction, similar to star arms. At longer time, the relaxed segments act as effective solvent because they do not contribute to stress (dynamic dilution effect) but do contribute to friction in the relaxation of the remaining stress-carrying segments. The relaxation of the inner backbone depends on its entanglement state.

Macromolecules with non-self-entangled backbones. After the relaxation of its branches, the relaxation of a non-self-entangled backbone of a comb macromolecule is well described by a Rouse process governed by the motion of the branches. In this case, backbone segments of increasing molar mass become disoriented and relax over time, until the relaxation time of the entire backbone becomes $\tau_{R,comb} = \tau_{branch} Z^2_{branch}$, in which τ_{branch} is the relaxation time of the branches and Z_{branch} is the number of branches attached to the backbone[32]. In this regime, G' and G'' exhibit a power-law dependence on frequency with an exponent of 1/2, characteristic of a Rouse process (Fig. 3a). Conversely, the relaxation of inner backbone of pompom-like macromolecules (Fig. 3c) is slightly different, because the branching points are only located at their extremities. Nevertheless, their relaxation proceeds through a Rouse process, at the rhythm of the disentanglement and re-entanglement dynamics of the branches, with which it is entangled[52]. Its characteristic relaxation time is the constraint release Rouse time $\tau_{CRR} = \tau_{branch} Z^2_{bb}$, in which Z_{bb} is the number of entanglements of the inner backbone.

Macromolecules with self-entangled backbones. The entangled backbone of a complex macromolecule relaxes via reptation and retraction processes similarly to a linear chain (Fig. 3b), but its relaxation time is substantially increased, owing to the additional friction coming from the branches[32,53–55]. Increasing the length of the branches and, consequently, their retraction time, increases the friction carried by each branching point and, therefore, delays the relaxation of the macromolecule (Fig. 3a). Nevertheless, this effect is counterbalanced by a dynamic dilution due to the branches, yielding a decrease of the

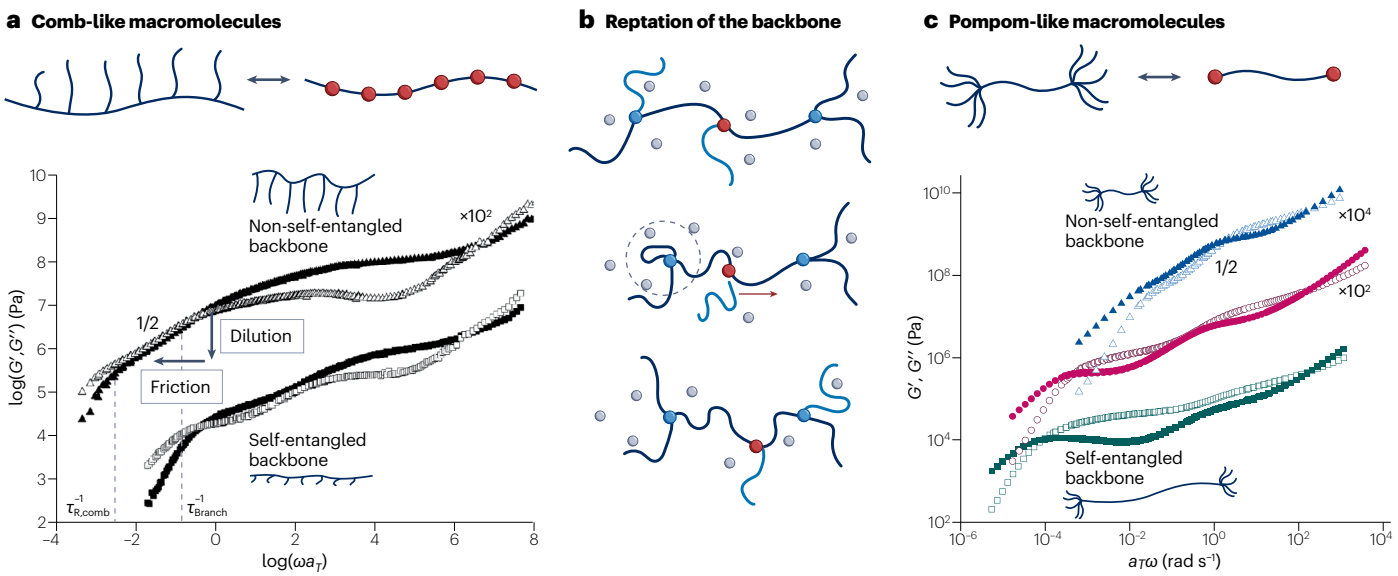


Fig. 3 | Rheological signatures of architecturally complex entangled macromolecules. a, Frequency (ω) dependent storage and loss moduli (G' and G'') for 1,4-polybutadiene comb melts. Master curves were obtained using time temperature superposition, by applying horizontal shift factors a_T determined from the Williams–Landel–Ferry (WLF) equation. The combs have the same number and different size of branches (larger on top with stronger dynamic dilution effect, the comb backbones being non-self-entangled and relaxing by a Rouse process at time $\tau_{R,comb}$). Relaxation occurs, first, by retraction of the branches at time τ_{Branch}. Top: at longer times, the branches act as friction points along the chain backbone. **b**, Schematic illustration of the hierarchical reptation of an entangled comb polymer: the inner backbone can diffuse but only if the branches are retracting to pass over the entanglements. **c**, Frequency dependent G' and G'' for pompom-like polystyrene melts with branches of molar mass 23 kg mol^{-1} and backbones of molar masses 100 kg mol^{-1} (non-self-entangled, blue), 220 kg mol^{-1} (red) or 400 kg mol^{-1} (green). Panel **a** adapted with permission from ref. 54, ACS. Panel **c** adapted from ref. 151, Springer Nature Limited.

original modulus of the network that is proportional to the square of the backbone concentration c^2 (refs. 5,6,30,31). This is reflected on a second, low-frequency plateau that emerges in the storage modulus. The dynamic dilution effect also speeds up the reptation time of the backbone, which must diffuse through an effectively 'fatter' tube that corresponds to fewer entanglements. Therefore, the relaxation of combs is controlled by two antagonistic effects that result from chain branching: an increased friction of the backbone and a faster reptation in a diluted environment.

Pompom polymers exhibit similar hierarchical relaxation. The low-frequency plateau modulus of the complex macromolecules is much lower than the initial rubbery plateau, due to the dilution effect of the branches, which can be seen by comparing the viscoelastic data of different pompom polymers that have similar friction coming from the branches (Fig. 3c). Increasing the weight fraction of the branches enhances their dilution effect and speeds up the backbone relaxation. By varying the number and the length of the branches, it is possible to adjust the contributions of these two antagonist effects and design molecular architectures to obtain desired rheological properties. Conversely, there are limited possibilities to tailor the rubbery plateau.

Networks based on dynamic intermolecular bonding

A powerful strategy to create transient polymer networks is by introducing physical (reversible) bonds (stickers) along polymeric chains (Fig. 4a) or at their extremities (Fig. 4d). The resulting networks exhibit viscoelastic properties arising from dynamic physical or chemical interactions that continuously form associations and break them over time. The lifetime of the stickers spans orders of magnitude, depending on the nature of the junctions, which range from hydrogen bonds and metal–ligand coordination to ionic interactions or dynamic covalent bonds[56–59]. Similar to the branches of a complex macromolecule, stickers act as effective frictional elements, which slow down the polymer chain relaxation. Drawing analogies between branched polymers and sticky chains is therefore useful for building a universal conceptual framework to describe the physics of macromolecular networks and engineer their properties. In the following, the sticker lifetime represents the time beyond which the transient network relaxes due to dissociation and association dynamics. This time is usually much larger than real association time of the reversible junctions, as it is expected that a sticker must dissociate and associate several times before hopping to a new position[60,61].

Linear viscoelasticity of transient networks built from sticky chains

Sticky chains with unentangled building blocks. The viscoelastic response of a representative unentangled sticky polymer is as follows (Fig. 4b). Starting from high frequency, a rubbery plateau in storage modulus is observed, with a value that is proportional to the number density of strands between two stickers (equation (2)). This network starts relaxing at time $t = \tau_{sticker}$, the sticker lifetime, which depends on the strength and stability of the bond (therefore, the type). This time, which is defined as the time at which the transient network starts relaxing through the dynamics of stickers, is usually far longer than the real association time of a single dynamic bond. Indeed, several inefficient association and dissociation steps between the same pair of stickers are expected to take place before a dissociated junction diffuses and creates a new bond. The sticker lifetime is thus a representative time,

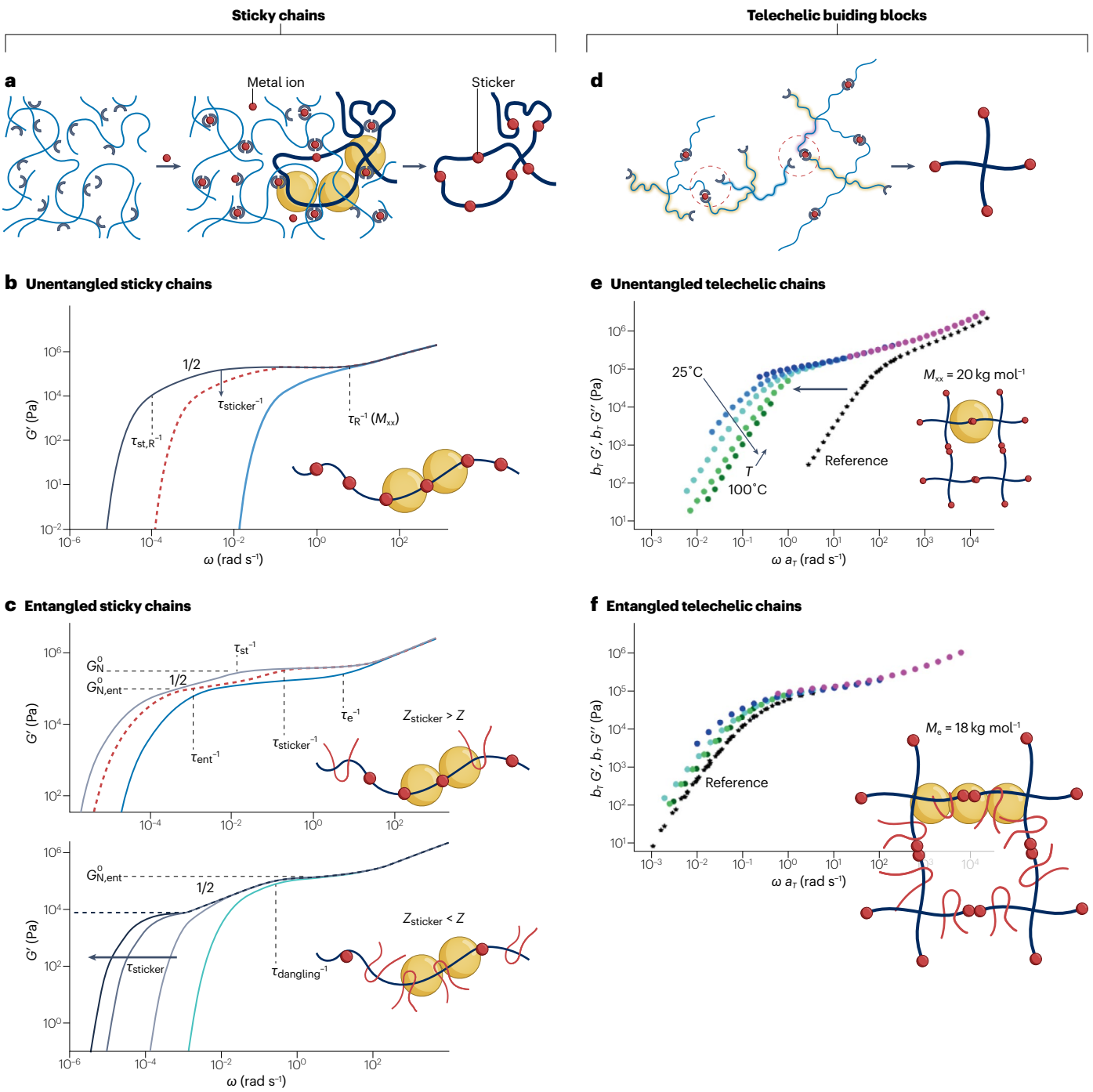


Fig. 4 | Sticky chains and telechelic building blocks (panels a, d). **a**,**d**, Sticky chains and telechelic building blocks. **b**–**d**, Schematical linear rheological response (storage modulus G') of sticky chains (**b**,**c**). The latter can be unentangled (panel **b**) or entangled (panel **c**), with a sticker density larger ($Z_{sticker} > Z$) or smaller ($Z_{sticker} < Z$) than the density of entanglements. The different curves correspond to the rheological responses for different sticker lifetime $\tau_{sticker}$, leading to different sticky Rouse time of the chain $\tau_{st,R}$ (**b**), to different sticky Rouse time of the entanglement segments τ_{ent} (panel **c**, top) or to different terminal relaxation time (**c**, bottom). Cartoon and frequency dependent G' for supramolecular networks obtained by adding Zn(II) ions to telechelic star poly(*n*-butyl-acrylate) melts end-functionalized by a terpyridine ligand (**d**). **e**,**f**, The building blocks are either unentangled, with an arm molar mass of 10 kg mol^{-1} per arm (**e**) or entangled, with a molar mass of 62 kg mol^{-1} (**f**). As the molar mass between two entanglements M_e is 18 kg mol^{-1}, both networks have the same mesh size (represented by the yellow sphere). The different curves represent the rheological responses at different temperatures. The temperature influence on the segmental dynamics has been taken into account through the horizontal shift factors a_T determined from the Williams–Landel–Ferry equation. Vertical shifts b_T have been applied to account for the temperature influence on the rubbery plateau (which reflects the product of density and temperature). Panels **e**,**f** adapted with permission from ref. 76, ACS.

which depends on both the nature of the bond and the time a sticker remains free, which may be coupled to the polymer chain relaxation[60,61]. The complete (terminal) relaxation of a sticky chain requires multiple dissociations and reassociations of the stickers to allow for the loss of segmental orientation (and structural memory) as the frequency decreases[60–62]. This process has been well described by the 'sticky Rouse model', with a terminal relaxation time $\tau_{st,R} = \tau_{sticker} Z^2_{stickers}$, in which $Z_{stickers}$ is the number of stickers along the chain. A characteristic of this process is the slope of 1/2 observed on G' and G'' in the frequency range between $1/\tau_{sticker}$ and $1/\tau_{st,R}$.

This model has been applied to diverse systems, including ionomers[11,63] and sticky chains associating via hydrogen bonding[64]. The viscoelastic behaviour of unentangled sticky chains can be compared with that of a comb polymer with an unentangled backbone, with the branches playing the same role as the stickers (Fig. 3a). The main difference between these two classes of macromolecular materials lies on the value of their rubbery plateau modulus: because the rubbery plateau of the comb polymer arises from the entanglements among branches, it cannot be tuned and moreover, it drops (often substantially, depending on the molecular characteristics) as soon as the branches relax, owing to the dynamic dilution effect coming from by the relaxation (disentanglement) of the branches (Fig. 3a). On the contrary, the rubbery plateau of sticky chains can be easily tailored by changing the density of stickers, something that does not lead to a dilution effect[65,66]. Hence, although both systems can be compared in terms of origin of friction and relaxation dynamics, comb polymers are much softer than sticky chains, and an increase in their relaxation time is always accompanied by a decrease of the elastic modulus[53,54].

Sticky chains with entangled building blocks. In this case, the transient network properties emerge from the interplay between two contributions: topological constraints (entanglements) and physical bonds (reversible junctions). Crucial challenges are to decode the relationship between the modulus of the rubbery plateau and the number densities of bonds (stickers) and entanglements and to identify the effect of the latter on the relaxation of entangled sticky chains. To rationalize their viscoelastic properties, it is convenient to classify these networks into two main categories, depending on whether the density of stickers is larger or smaller than the density of entanglements.

Sticky chains containing a high number density of stickers usually display two rubbery plateau regimes[67,68] (Fig. 4c). The first, at high frequencies, arises from the contribution of both types of physical bonds (equation (4)) and extends up to the lifetime of the stickers, where a sticky Rouse process takes place. That process ends at the relaxation time of the entanglement segments, $\tau_{ent} = \tau_{sticker} Z^2_{st,e}$ ($Z_{st,e}$ is the number of stickers between two entanglements), where a second rubbery plateau regime is observed, arising solely from the contribution of the entanglements and characterized by a modulus $G^0_{N,ent}$. To further relax, the chains must diffuse through their entanglements, which is only possible through many dissociation and association steps of the stickers. This slow diffusion process is well described by the sticky reptation model[12]. In this model, the reference microscopic time of an entanglement segment is its sticky Rouse time, τ_{ent}, rather than its intrinsic Rouse time, τ_e, typically used for entangled chains. For specific systems with fast sticker dynamics, the friction from the backbone itself may become non-negligible compared with the friction from the stickers. In such cases, both contributions must be accounted for to describe the chain diffusion.

The relaxation of sticky chains containing a low number density of stickers can be rationalized in the context of the relaxation of entangled comb macromolecules. At short times, only the dangling ends that are not trapped between two sticky junctions can disentangle and relax[12]. Subsequently, a second rubbery plateau is observed, due to the entangled chain segments trapped between two stickers (Fig. 4c). Then, at times $t \gg \tau_{sticker}$, the chain relaxes by a reptation process that is slowed down by the extra friction arising from the stickers, and the terminal regime of relaxation is reached. Again, the main difference between sticky chains and comb polymers is the importance of the dilution effect: for sticky chains, only the dangling ends contribute to the dilution of the network, whereas for comb polymers all branches are involved, which represent an important fraction of the polymer and which substantially reduce the storage modulus.

Influence of temperature. This marks another important difference between sticky and comb polymers. The temperature dependence of the relaxation time of a comb polymer is well described by the Williams–Landel–Ferry (WLF) equation for the horizontal shift factor a_T: $\log a_T = -\frac{C_1(T-T_{ref})}{C_2+(T-T_{ref})}$, in which T is temperature, T_{ref} is the reference temperature for shifting the data along the frequency axis, and C_1 and C_2 are material constants[69]. Typically, there is a tiny vertical shift factor (b_T) along the moduli axis, which reflects the variation of density with temperature, as demonstrated for nonionic linear and branched polymers[49,51,54], for example. However, for more complex polymeric materials, such as associating polymers, an increase of temperature may provide the necessary activation energy for bond break-up, hence substantially reducing the plateau modulus, which translates to a larger vertical shift factor[70,71]. The shift factors are used to construct linear viscoelastic master curves based on the principle of time–temperature superposition.

Conversely, the lifetime of the reversible junctions usually follows an Arrhenius dependence on temperature, in addition to the WLF behaviour of the chain backbone itself. This difference offers interesting paths to tune the properties of sticky chains. For example, it is possible to adjust the friction from the stickers (Arrhenius-like) and that from the chain backbone itself (WLF-like) in the chain reptation process, leading to a thermorheologically complex network. Moreover, if the density of stickers is low enough to form complex macromolecular assemblies that entangle with each other, rather than a percolated network, their relaxation could follow one of two paths: a sequence of dissociation dynamics of the stickers and disentanglement of the backbone or a disentanglement of the macromolecular assemblies. The faster process, which depends on temperature, is the one that dominates.

Thus, although the relaxation time of transient network formed by sticky chains strongly depends on the sticker lifetime, it also depends on the number of stickers per chain and on the entanglement state of the latter. This leads to rich rheological behaviour tunable through chemistry, molecular design and temperature. Last but not least, it should be mentioned that the composition (for example, the catalyst used or the nature and concentration of small crosslinkers) plays an important role on the thermorheological response of associating networks and has been used as a parameter to construct the linear viscoelastic master curves via time–temperature–catalyst superposition or time–temperature–crosslinker type superposition[72,73].

Linear viscoelasticity of transient networks from telechelic building blocks

Chains with sticky groups at their extremities represent telechelic building blocks that also form transient networks. As an example, Fig. 4e,f

shows the linear viscoelastic response of unentangled telechelic star molecules whose arms are end-terminated by a terpyridine ligand[74,75]. When metal ions are added to the sample, reversible junctions are created between the stars via metal–ligand coordination, and a polymeric network is obtained with a rubbery plateau modulus that is proportional to the number density of junctions (equation (2)). The respective terminal relaxation time is controlled by the dissociation dynamics of the stickers. The activation energy determined from the Arrhenius temperature dependence of the terminal regime is therefore equivalent to the activation energy that corresponds the temperature dependence of the sticker lifetime[74–77].

However, this direct relationship is usually lost in the case of transient networks built from entangled telechelic building blocks (Fig. 4f): their relaxation requires both sticker dissociation and the retraction of the unassociated arms. Depending on the relative importance of these two processes (that is, sticker lifetime compared with retraction time of a free arm, τ_{arm}), the temperature dependence of the terminal relaxation time of the network can vary from Arrhenius (if $\tau_{sticker} \gg \tau_{arm}$) to WLF (if $\tau_{sticker} \ll \tau_{arm}$), allowing modulation of the influence of temperature on the viscoelastic response of these networks.

Considering the role of additional friction, the properties of these telechelic systems can be compared with the relaxation of linear or star polymers bearing branches at their extremities. However, their storage modulus does not exhibit two plateau regimes as in the case of pompom macromolecules, because there is no dilution effect. Moreover, despite the fast relaxation of the unentangled building blocks, a rubbery behaviour can be achieved with the corresponding transient network that is unable to relax before $t = \tau_{sticker}$. Hence, such a sharp transition between rubber-like and liquid-like behaviour cannot be obtained with complex architectures.

Nonlinear viscoelasticity of complex macromolecules and transient networks

Response in uniaxial extension (elongation)

Unlike linear and star polymer melts, complex macromolecules and transient networks undergoing elongation typically exhibit substantial strain (or extension) hardening. They also exhibit extension thickening (that is, increase of steady-state extensional viscosity with increasing extensional rate) at moderately high strain rates.

Complex architectures. At Hencky strain rates exceeding the inverse relaxation time of the outer branches, the branching points cannot freely diffuse, because the drag force is too strong to allow the chain to go back to its equilibrium state. Consequently, the backbone is stretched and strain hardens (Fig. 5a,b). There is a continuous increase of stretching with time until a maximum stretch value is reached[78]. This value corresponds to the stretch at which the monomeric tension along the backbone is so large that it counterbalances the effect of the drag force on the chain branching points[78–82]. As an example, for a pompom molecule the maximum stretch that the inner backbone can withstand is equal to the number of branches attached to the branching points[83]. Besides the role of the number of branches, strain hardening can also be modulated by varying the length of the branches, which affects the mobility of the branching point and, thus, the equilibration time of the backbone[37,79,80,83] (Fig. 5a). The finite extensibility of the network strands, which depends on the network mesh size (or, here, on the length of the inner backbone) is also an important parameter. In general, extension hardening is enhanced as the number of entanglements of the inner backbone increases (Fig. 5).

Transient networks. A similar strain hardening behaviour is also obtained with associating polymers[84–86]. If the elongation strain rate is larger than the inverse sticker lifetime, the transient networks respond similarly to chemical networks, with the monomeric tension along the network strands increasing with time (strain). However, because the associative moieties represent the weaker bonds of the network, they break if the tension in the network strands exceeds a certain threshold[81,87–89]. This threshold sets the maximum stretch level of the associating networks and depends on the nature of the transient bonds, that is, the strength they can withstand before breaking. The maximum stretch level also depends on the length of the network strands. Shorter strands reach their maximum extensibility at smaller strain deformation (Fig. 5c), which leads to premature breakage of the network. Once a junction is dissociated, it can form a new bond or remain dissociated, depending on the strain rate. In the latter case, the sample exhibits a brittle behaviour. In the case of unentangled sticky chains, a brittle to ductile transition as a function of the density and lifetime of the stickers occurs (Fig. 5d). The deformability of the transient networks strongly depends on the maximum stretch the network strands can accommodate before rupture[86]. The critical stretch ratio for macroscopic fracture of the material is $\sqrt{N_s}$, in which N_s is the number of Kuhn segments per strand (this value can be smaller if there is finite extensibility[86,90,91]). Moreover, the brittleness of the networks depends on the sticker lifetime and its relative importance compared with the Rouse time of the precursor chains. Indeed, once a junction is broken, a very fast retraction of the chain, compared with the sticker dynamics, promotes the formation of defects or microscopic cracks[91,92]. The lifetime of the stickers may also be force dependent, a fact that must be accounted for to explain the influence of the deformation rate on the fracture behaviour of the transient network[93].

Maximum stretch ratio. At high extensional rates, a steady state is reached when the stretch factor reaches its maximum value. For complex macromolecules, this maximum stretch ratio (with respect to the equilibrium size) corresponds to the stretch at which the monomeric tension along the backbone counterbalances the force needed for branch point withdrawal. In the case of a dynamic network, it corresponds to the stretch value at which the transient bonds dissociate.

Role of the entanglements. For both branched architectures and transient networks, entanglements play a unique role: although under elongation at short times they contribute to the network elasticity (equation (4)), their influence becomes negligible in the steady-state regime[79,80,82,83,94]. For example, two networks that have similar mesh size, originating either from supramolecular junctions or from both supramolecular junctions and entanglements (Fig. 5c), exhibit a similar behaviour in the linear regime (Fig. 4e,f) and at short times under elongation, but the entangled network has a much larger extensibility compared with the network based on unentangled building blocks. This difference has been attributed to the ability of the chains to slide through these entanglements and equilibrate their tension on a larger length scale (M_{xx}) compared with the entanglement molar mass M_e. Consequently, the contribution of entanglements to the critical stretch ratio for macroscopic fracture is very small, leading to much higher extensibility.

Role of the fast-relaxing dangling arms. Except at very high deformation rate, dangling ends do not stretch. Their contribution to the extensional stress growth coefficient (transient viscosity) $\eta^+(t)$ vanishes at

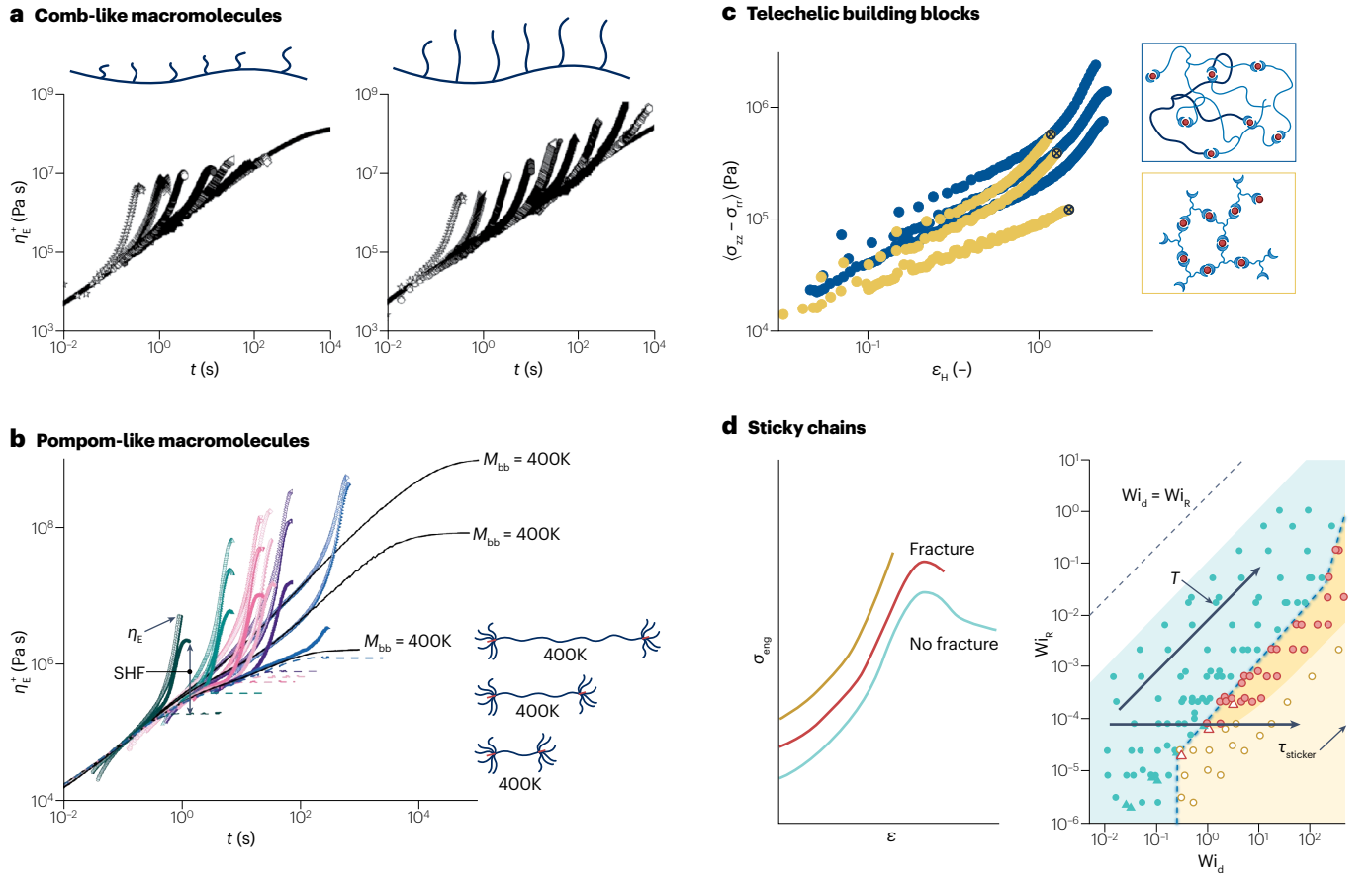


Fig. 5 | Response to elongation. a, Transient stress $\eta^+(t)$ (also called stress growth coefficient) as a function of time t for the comb polymers with branches of increasing length shown in Fig. 3. **b**, Behaviour of the pompom macromolecules shown in Fig. 3. The importance of strain hardening (represented by the strain hardening factor (SHF)) increases with the molar mass of the inner backbone (M_{bb}). **c**,Evolution of the extensional stress difference between the axial (σ_{zz}) and radial (σ_{rr}) direction of the telechelic star polymers shown in Fig. 4e,f. The crosses represent sample breakage. **d**, Engineering extensional of unentangled sticky chains. The diagram shows regimes of fracture in terms of Weissenberg number based on Rouse time (Wi_R) versus Weissenberg number based on terminal time (Wi_d). The orange shaded area represents the regime of brittle fracture that occurs when the transient elongational stress reaches values before and after the overshoot. Whereas at strain rates $\dot{\varepsilon} < 1/\tau_{rel}$ the broken reversible junctions can rearrange and reform before fracture takes place, at higher rates fracture occurs if the sticker lifetime is much larger than the Rouse time of the precursor. Panel **a** adapted with permission from ref. 82, AIP. Panel **b** adapted from ref. 151, Springer Nature Limited. Panel **c** adapted with permission from ref. 94, ACS. Panel **d** adapted with permission from ref. 91, ACS.

short time, equal to their relaxation time. If their relaxation is fast, the strain hardening of the inner backbone is visible earlier (Fig. 5b), leading to an enhanced strain hardening factor (the ratio of the value of the transient elongational response $\eta^+(t)$ at a given stretch rate to the respective value in the linear viscoelastic regime $\eta_{LVE}(t)$). Nevertheless, the (long-time) steady-state value of the viscosity is not affected by this effect[33].

Response in shear

Complex architectures (Fig. 6a,b) and associative unentangled systems (Fig. 6c) behave very differently under strong shear flow. Transient networks from unentangled telechelic building blocks can display strong transient shear strain hardening at shear rates larger than their inverse sticker lifetime (Fig. 6c). This phenomenon has been attributed to the inability of the network strands to relax their stretch at the experimental time and the associated resistance of the junctions[74,95]. Similar behaviour has been observed with wormlike surfactant micelles[96] and supramolecular polymers built from hydrogen-bonding moieties[97]. Moreover, although at low shear rates the viscoelastic response of a transient network strongly depends on the lifetime of the stickers, at high shear rates the nature of the sticker has only a small influence. Strain-induced break-up of the reversible junctions is observed when the network strands reach a critical stretch, leading to a constant yield strain independently from the imposed shear rate and sticker strength[95,98]. However, this critical stretch and extent of the overshoot depend on the molar mass of the strands between two crosslinking points (Fig. 6d). Such transient hardening is very rarely observed in entangled complex macromolecules[99]. Typically, a strain softening response is seen, with the overshoot in transient viscosity (stress) marking the maximum deformation before orientation and disentanglement[100]. This is qualitatively identical to the response of entangled linear polymers[8,101] (Fig. 2d). Nevertheless, the signature of the branches is distinct as, depending on their number and molar mass, they contribute to the broadness of the overshoot and even the

appearance of a double overshoot (one associated with the branches and one with the backbone)[102,103]. Shear start-up data for comb and H polystyrenes reveal strain softening, a broad overshoot and even a weak undershoot (attributed to chain tumbling) on increasing shear rate[55] (Fig. 6a,b).

Dual and double networks combining two types of associations

Double networks combine two different types of bonds in one network and have yielded tunable materials[104,105]. Typically, the first bond is permanent or has an extremely long lifetime, and the second is physical, with a much shorter association lifetime. The strong and weak bonds can be located at the same chain, forming a dual network (Fig. 7a) or at different chains, forming interpenetrated networks (Fig. 7b). The weaker bond is called sacrificial and is the first one to break under elongation, whereas the second, very loosely crosslinked network, ensures large extensibility of the sample[106,107]. The elastic modulus of these materials is larger than the sum of the moduli of the single networks (equation (4)), because their entanglements also contribute to the sample elasticity[68,108]. These entanglements trapped in the network are potentially crucial for force transmission between the two networks. They also ensure complete recovery after a creep test[109] (Fig. 7d). Hence, the unique trade-off of mechanical stiffness and deformability in this class of materials originates from the synergic effect of these two types of bonds, providing large mechanical modulus (strong bonds) and enhanced ductility. Such behaviour is also observed in nature. For example, marine mussels are composed of collagen decorated with proteinaceous cuticles, forming iron-catechol complexes that provide the necessary mechanical properties to survive the wave-swept intertidal zone. This observation has led to the development of biomimetic double networks[110–114]. In general, the dynamics of such networks at different scales can be described using the sticky Rouse and sticky reptation models. The relaxation processes, which reflects the two bonds, can be modulated by tailoring the length of the chains, the density and strength (equivalently, lifetime) of the stickers and, for interpenetrated networks, the composition of the networks. This provides control over network properties such as shape memory, self-healing and strength[106,110,113,115].

A design challenge in entangled interpenetrated networks is to tailor the bond lifetime in relation to disentanglement process. For example, if both the strong and the weak bonds dissociate and associate many times before the building blocks disentangle, an average

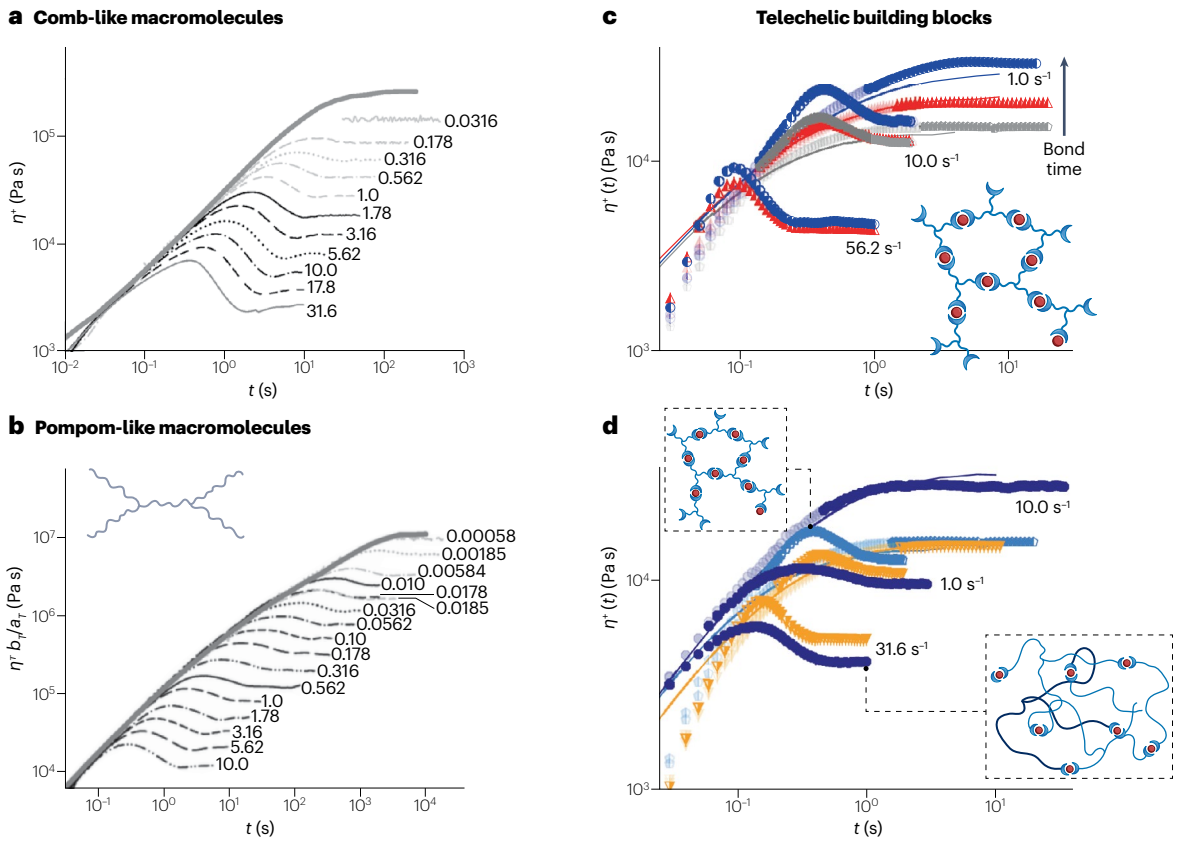


Fig. 6 | Transient shear viscosities $\eta^+(t)$. a–**d**, A polystyrene comb (**a**) and a polystyrene H melt (schematically illustrated) resembling a pompom (**b**) at different shear rates (increasing from top to bottom) as marked on the plots. Influence of the bond lifetime on the transient shear viscosity of networks with unentangled telechelic poly(*n*-butyl acrylate) star building blocks (**c**). The networks contain Zn(II) ions at 25 °C (red triangles), a blend of Zn(II) and Cu(II) ions at 40 °C (blue circle) or Cu(II) ions at 60 °C (grey pentagon). Influence of the molar mass of the precursor on the transient shear viscosity of networks with telechelic star building blocks and Cu(II) ions at 60 °C (**d**). The molar mass of the star arms is 10 kg mol^{-1} (grey circles), 13 kg mol^{-1} (yellow triangles) or 62 kg mol^{-1} (blue circles)[76]. Panel **a** adapted with permission from ref. 100, AIP. Panel **b** adapted with permission from ref. 55, AIP. Panels **c**,**d** adapted with permission from ref. 94, ACS.

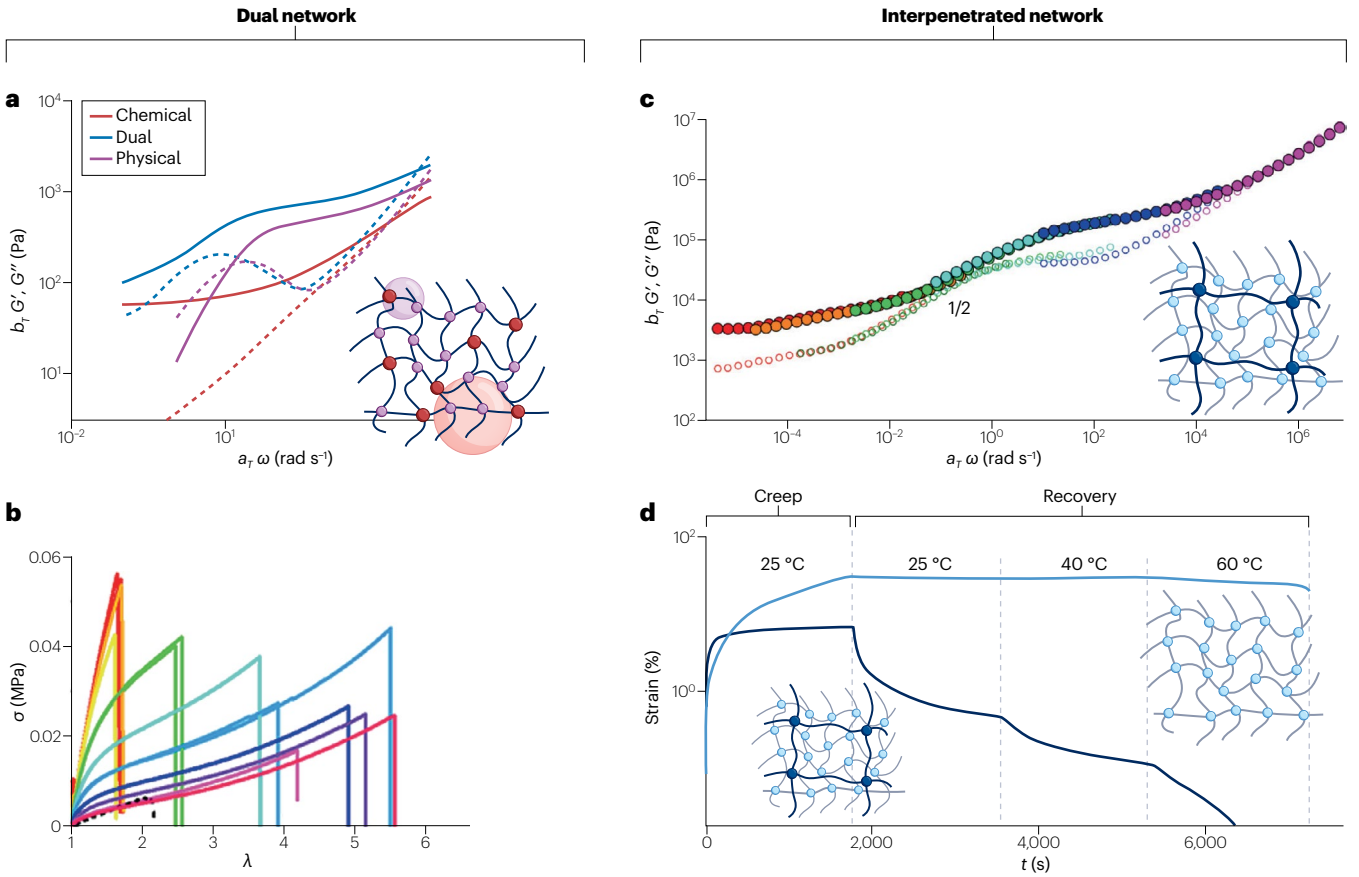


Fig. 7 | Dual and interpenetrated networks. a, Angular frequency dependence of storage and loss moduli G' (solid lines) and G'' (dashed lines) of the poly(vinyl alcohol) chemical, physical and dual crosslink gel. The temperature influence on the segmental dynamics has been taken into account by applying horizontal shift factors a_T determined from the Williams–Landel–Ferry equation. Vertical shift factors b_T have been applied to account for the temperature dependence of the rubbery plateau modulus (product of density and temperature). **b**, Tensile stress (σ) versus strain (λ) curves for the dual crosslink gels at various initial strain rates, from low (magenta) to high rates (yellow and red). For the comparison, the curve for the chemical gels at an initial strain rate of 0.03 s^{-1} (dashed line) is also shown. **c**, Master curves of the storage (filled symbols) and loss (empty symbols) moduli for a double network composed of a (weak) metallo-supramolecular network built from sticky poly(*n*-buthyl-acrylate) reference sample of molar mass 27 kg mol^{-1}, in the presence of Zn(II) ions and a (strong) vitrimers network, at temperature T_{ref} = 25 °C. The data have been measured at T from −20 °C (magenta) to 100 °C (red) and have been shifted either by the Williams–Landel–Ferry equation at high frequency or an Arrhenius equation at low frequency. **d**, Creep-recovery curves (relative strain) of the metallo-supramolecular network (light blue), compared with its response if an interpenetrated vitrimer network is added (dark blue, dashed-dotted curve). The applied stress is 1,000 Pa. Creep temperature is 25 °C, whereas the recovery temperature is first fixed at 25 °C (from 1,800 to 3,600 s), then at 40 °C and then increased by steps of 20 °C every 30 min. Panel **a** adapted with permission from ref. 117, ACS. Panel **b** adapted with permission from ref. 116, ACS. Panel **c** adapted with permission from ref. 152, AIP.

effect of their contribution is observed, leading to a single-step relaxation. Conversely, if the disentanglement time is fast compared with the sticker dissociation time, a two-step relaxation of the network occurs. Therefore, selecting sticker–polymer combinations enables achievement of desired properties.

Double networks usually have two rubbery plateau regimes in their linear viscoelasticity data, arising from both types of stickers at short time and only from the long lifetime stickers at long time (Fig. 7c). Their nonlinear shear response bears analogies with that of complex architectures discussed above, for example, in the case of two bonds of different strengths, a double transient viscosity overshoot may appear[95].

In the nonlinear regime, the viscoelastic response strongly depends on the applied strain rate, compared with the lifetime of the two types of stickers. If it is faster than the inverse lifetime of both types of stickers, the network behaves as a permanently bonded network, with high elastic modulus and low strain at break[116] (Fig. 7b). However, if the network is deformed much slower than the rate at which the fast stickers dissociate and reassociate, the contribution of the fast bonds on the stress–strain response of the network is nearly negligible, leading to a soft and extensible network. There is an optimal stretch ratio or lifetime between the slow and the fast stickers, in which continuous dissociation and association of the weaker bonds delay the chain retraction after the strain-induced break-up of the stronger junctions, thereby suppressing the formation of defects (or microscopic cracks) that are thought to yield macroscopic fracture[116,117].

Finally, double dynamics networks can be obtained from telechelic molecules that have two different types of bonds at their extremities[76,95]. Depending on their lifetime compared with the disentanglement time of the building blocks, a two-step relaxation of the network can be observed, or a single-step one, occurring at times

between the lifetime of the two types of stickers. This behaviour suggests that the stickers must dissociate and associate many times before the relaxation of the building blocks. Understanding the influence of the ratio between disentanglement time and stickers lifetime allows selecting sticker–polymer combinations to achieve desired properties. Under nonlinear shear flow, these double networks may exhibit two overshoots in their transient signal, each associated with one bond.

Outlook

By correlating molecular characteristics with macroscopic properties and appreciating and exploiting the analogy between branched and associating polymers, criteria for molecular design of polymer networks with desired mechanical properties could be developed.

Networks with sliding junctions

Sliding junctions, such as slide-rings, represent delocalized weak constrains similar to entanglements[118]. Networks based solely on slide-rings behave similarly to linear entangled chains, but combined with another type of junctions as described above, they can become strong double networks. Their advantage is the ability to tailor the lifetime of the strong bonds (hence, network elasticity), while allowing sliding (hence, local dissipation)[119]. Their resulting properties in the direction of combining stiffness, deformability and flow may offer new features (in view of the sliding nature of the weak junctions at large deformations) that have not yet been exploited[120].

Networks based on bottlebrushes

The central framework to discuss the properties of networks presented above can be used to understand networks formed from bottlebrush homopolymers or copolymers. Bottlebrushes are densely grafted comb polymers, with elastic and flow properties that can be modulated by varying grafting density and size of grafted arms. They are efficient building blocks for soft elastomers with molecularly adaptive properties mimicking those of biological tissues[121–123]. The new degrees of freedom here for molecular design are grafting density and, for copolymers, self-assembly (driven by the predominance of enthalpic interactions).

Vitrimers

This unique class of polymeric networks is characterized by fast-exchange bonding and debonding reactions (using dynamic covalent bond chemistry), which maintain the junction density (hence, network elasticity) constant for a long time before eventual flow (often facilitated by heating). This feature makes vitrimers malleable materials that encompass short-time thermosetting and long-time thermoplastic behaviour[124–126]. Operationally, they are one-type associating polymers that are often impossible to dissolve in a reasonable experimental time. They have been proposed as effective compatibilizers of immiscible polymer blends, with potential applications in recycling processes[127], and there has been much recent work on compatibilizing immiscible plastics using vitrimers[128–134]. A challenge for design and applications is the possibility of microphase separation due to chemically different nature of bonding groups and the polymeric segments; this challenge draws analogies to the much-studied block copolymers[135–137].

Nanocomposites and macromolecular architecture

This class of filled networks offers tunability of properties by selecting polymeric matrices of different molar mass and particles of different shape, size and surface treatment. The big picture is that of substantial reinforcement, especially when the fillers (added nanoparticles) form different types of structures by means of self-assembly[137–139]. Application of a shear field improves particle dispersion and reduces elasticity (the Payne effect)[140]. Both particle interaction and chain entanglement contribute to these effects. Combining with macromolecular architecture may offer additional possibilities to fabricate materials with desired tunable properties.

Controlling the spatial distribution of functional groups

The framework discussed in this Review is general, but in terms of associating networks, examples from randomly placed or telechelic stickers have been shown. An important molecular parameter that affects the properties of associating networks is the spatial distribution of the sticky groups. This can be controlled with good accuracy by taking advantage of advanced modern polymer chemistry approaches. Hence, chemistry (both synthesis of polymers and placement of specific functional groups) is a useful tool to tune the thermorheological behaviour of polymeric networks with reversible associations[141–145].

Published online: 25 September 2026

References

1. Meyer, K. H. et al. Die elastischen eigenschaften der organischen hochpolymeren und ihre kinetische deutung. *Kolloid Z.* **59**, 208–216 (1932).
2. Guth, E. & Mark, H. Zur innermolekularen, statistik, insbesondere bei kettenmolekiilen I. *Monatsh. Chem.* **65**, 93–104 (1934).
3. Green, M. S. & Tobolsky, A. V. A new approach to the theory of relaxing polymeric media. *J. Chem. Phys.* **14**, 80–92 (1946).
4. Doi, M. & Edwards, S. F. *The Theory of Polymer Dynamics* (Oxford Univ. Press, 1986).
5. Graessley, W. W. *Polymer Liquids and Networks: Structure and Properties* (Garland Science, 2004).
6. Rubinstein, M. & Colby, R. H. *Polymer Physics* (Oxford Univ. Press, 2003).
7. Podara, C. et al. Recent trends of recycling and upcycling of polymers and composites: a comprehensive review. *Recycling* **9**, 37 (2024).
8. Dealy, J. M., Read, D. J. & Larson, R. G. *Structure and Rheology of Molten Polymers: From Structure to Flow Behavior and Back* 2nd edn (Hanser, 2018).
9. Milner, S. T. & McLeish, T. C. B. Parameter-free theory for stress relaxation in star polymer melts. *Macromolecules* **30**, 2159–2166 (1997).
10. Ball, R. C. & McLeish, T. C. B. Dynamic dilution and the viscosity of star polymer melts. *Macromolecules* **29**, 5717–5772 (1989).
11. Chen, Q. et al. Ionomer dynamics and the sticky rouse model. *J. Rheol.* **57**, 1441–1462 (2013).
12. Leibler, L. et al. Dynamics of reversible networks. *Macromolecules* **24**, 4701–4707 (1991).
13. Hawke, L. G. D. et al. Viscoelastic properties of linear associating poly(*n*-butyl acrylate) chains. *J. Rheol.* **60**, 297–310 (2016).
14. Yang, Y. et al. Polyelectrolyte complex-covalent interpenetrating polymer network hydrogels. *Macromolecules* **53**, 6956–6967 (2020).
15. Daniel, W. F. M. et al. Solvent-free, supersoft and superelastic bottlebrush melts and networks. *Nat. Mater.* **15**, 183–189 (2016).
16. Huang, Q. et al. Unexpected stretching of entangled ring macromolecules. *Phys. Rev. Lett.* **122**, 208001 (2019).
17. O'Connor, T. C. et al. Topological linking drives anomalous thickening of ring polymers in weak extensional flows. *Phys. Rev. Lett.* **124**, 027801 (2020).
18. Sorichetti, V. et al. Effect of chain polydispersity on the elasticity of disordered polymer networks. *Macromolecules* **54**, 3769–3777 (2021).
19. Huang, J. et al. Ultrahigh energy-dissipation elastomers by precisely tailoring the relaxation of confined polymer fluids. *Nat. Commun.* **12**, 3610 (2021).
20. Gu, Y. et al. Polymer networks: from plastics and gels to porous frameworks. *Angew. Chem. Int. Ed.* **59**, 5022–5049 (2020).
21. Zhang, S. et al. Elastomer mechanics of cross-linked linear-ring polymer melts. *ACS Macro Lett.* **14**, 509–515 (2025).
22. Brassine, S. et al. Dissociating sticker dynamics from chain relaxation in supramolecular polymer networks—The importance of free partner! *J. Rheol.* **61**, 1123–1134 (2017).
23. Borger, A. et al. Threading–unthreading transition of linear-ring polymer blends in extensional flow. *ACS Macro Lett.* **9**, 1452–1457 (2020).
24. Liu, S. & O'Connor, T. C. Flow-driven stretch fluctuations govern the nonlinear viscoelasticity of elongating associative polymer networks. *Phys. Rev. Lett.* **135**, 098101 (2025).
25. Barzycki, D. C. et al. Linear viscoelasticity of polystyrene vitrimers: segmental motions and the slow Arrhenius process. *Macromolecules* **58**, 3949–3963 (2025).
26. Nechmad, N. B. et al. Reimagining polymer networks from molecule to material. *Macromolecules* **58**, 12909–12930 (2025).

27. Merti, V. et al. Physical networks from multifunctional telechelic star polymers: a rheological study by experiments and simulations. *Macromolecules* **51**, 2872–2886 (2018).
28. Soman, B. Effect of precise linker length, bond density, and broad temperature window on the rheological properties of ethylene vitrimers. *Soft Matter* **17**, 3569–3577 (2021).
29. Burger, N. A. et al. High-pressure effects on gelatin sol–gel transition. *Ind. Eng. Chem. Res.* **64**, 7370–7380 (2025).
30. Danielsen, S. P. O. Molecular characterization of polymer networks. *Chem. Rev.* **121**, 5042–5092 (2021).
31. Marrucci, G. Relaxation by reptation and tube enlargement: a model for polydisperse polymers. *J. Polym. Sci. Polym. Phys. Ed.* **23**, 1590177 (1985).
32. McLeish, T. C. B. Tube theory of entangled polymer dynamics. *Adv. Phys.* **51**, 1379–1527 (2002).
33. Huang, Q. et al. Dynamics of star polymers in fast extensional flow and stress relaxation. *Macromolecules* **49**, 6694–6699 (2016).
34. O'Connor, T. C. et al. Relaxation in highly oriented melts of entangled polymers. *Macromolecules* **52**, 8540–8550 (2019).
35. O'Connor, T. C. et al. Relating chain conformations to extensional stress in entangled polymer melts. *Phys. Rev. Lett.* **121**, 047801 (2018).
36. Bach, A. et al. Elongational viscosity of narrow molar mass distribution polystyrene. *Macromolecules* **36**, 5174–5179 (2003).
37. Huang, Q. When polymer chains are highly aligned: a perspective on extensional rheology. *Macromolecules* **55**, 715–727 (2022).
38. Matsumiya, Y. & Watanabe, H. Non-universal features in uniaxially extensional rheology of linear polymer melts and concentrated solutions: a review. *Prog. Polym. Sci.* **112**, 101325 (2021).
39. Matsumiya, Y. et al. Nonlinear elongational rheology of unentangled polystyrene and poly (*p-tert*-butylstyrene) melts. *Macromolecules* **51**, 9710–9729 (2018).
40. Morelly, S. L. et al. Effect of finite extensibility on nonlinear extensional rheology of polymer melts. *Macromolecules* **52**, 915–922 (2019).
41. Huang, Q. et al. Concentrated polymer solutions are different from melts: role of entanglement molecular weight. *Macromolecules* **46**, 5026–5035 (2013).
42. Shahid, T. et al. Diluting entangled polymers affects transient hardening but not their steady elongational viscosity. *Macromolecules* **52**, 2521–2530 (2019).
43. Xu, X. et al. Shear thinning behavior of linear polymer melts under shear flow via nonequilibrium molecular dynamics. *J. Chem. Phys.* **140**, 174902 (2014).
44. Parisi, D. et al. Nonlinear shear rheology of entangled polymer rings. *Macromolecules* **54**, 2811–2827 (2021).
45. Xu, Z. et al. Nature of steady-state fast flow in entangled polymer melts: chain stretching, shear thinning, and viscosity scaling. *Macromolecules* **55**, 10737–10750 (2022).
46. Dalne, M. et al. Nonlinear shear rheology of unentangled polymer melts. *Macromolecules* **58**, 7062–7083 (2025).
47. McLeish, T. C. B. et al. Dynamics of entangled H-polymers: theory, rheology, and neutron-scattering. *Macromolecules* **32**, 6734–6758 (1999).
48. Roovers, J. Melt rheology of H-shaped polystyrenes. *Macromolecules* **17**, 1196–1200 (1984).
49. Kapnistos, M. et al. Linear rheology of comb polymers with star-like backbones. *Rheol. Acta* **46**, 273–286 (2006).
50. Blackwell, R. J. et al. Theoretical linear and nonlinear rheology of symmetric treelike polymer melts. *Macromolecules* **34**, 2579–2596 (2001).
51. van Ruymbeke, E. et al. Viscoelasticity and extensional rheology of model Cayley-tree polymers of different generations. *J. Rheol.* **54**, 643–662 (2010).
52. Lentzakis et al. Constraint release mechanisms for H-polymers moving in linear matrices of varying molar masses. *Macromolecules* **52**, 3010–3028 (2019).
53. Ahmadi, M. et al. Time marching algorithm for predicting the linear rheology of monodisperse comb polymer melts. *Macromolecules* **44**, 647–659 (2011).
54. Kapnistos, M. et al. Linear rheology of architecturally complex macromolecules: comb polymers with linear backbones. *Macromolecules* **38**, 7852–7862 (2005).
55. Snijkers, F. et al. Start-up shear flow of a well-characterized entangled H-polymer. *Eur. Polym. J.* **206**, 112806 (2024).
56. Zhang, Z. et al. Dynamics of associative polymers. *Soft Matter* **14**, 2961–2977 (2018).
57. Wu, S. & Chen, Q. Advances and new opportunities in the rheology of physically and chemically reversible polymers. *Macromolecules* **55**, 697–714 (2021).
58. Yan, T. et al. What controls the structure and the linear and nonlinear rheological properties of dense, dynamic supramolecular polymer networks? *Macromolecules* **50**, 2973–2985 (2017).
59. Tang, J. et al. Revisiting the tensile behavior of dual cross-linked poly (vinyl alcohol) gel. *Macromolecules* **58**, 6617–6623 (2025).
60. Rubinstein, M. & Semenov, A. N. Thermoreversible gelation in solutions of associative polymers. 2. Linear dynamics. *Macromolecules* **31**, 1386–1397 (1998).
61. van Ruymbeke, E. et al. Rheology and structure of entangled telechelic linear and star polyisoprene melts. *Macromolecules* **43**, 4401–4411 (2010).
62. Rubinstein, M. & Semenov, A. N. Dynamics of entangled solutions of associating polymers. *Macromolecules* **34**, 1058–1068 (2001).
63. Chen, Q. et al. Viscoelasticity of reversible gelation for ionomers. *Macromolecules* **48**, 1221–1230 (2015).
64. Verjans, J. et al. Physically crosslinked polyacrylates by quadruple hydrogen bonding side chains. *J. Mater. Chem. B* **12**, 12378–12389 (2024).
65. Koziol, M. F. et al. Hierarchy of relaxation times in supramolecular polymer model networks. *Phys. Chem. Chem. Phys.* **24**, 4859–4870 (2022).
66. Ricarte, R. G. & Shanbhag, S. Unentangled vitrimer melts: interplay between chain relaxation and cross-link exchange controls linear rheology. *Macromolecules* **54**, 3304–3320 (2021).
67. Chen, Q. et al. Viscoelasticity of entangled random polystyrene ionomers. *J. Rheol.* **60**, 1031–1040 (2016).
68. Ge, S. Polymer architecture dictates multiple relaxation processes in soft networks with two orthogonal dynamic bonds. *Nat. Commun.* **14**, 7244 (2023).
69. Ferry, J. D. *Viscoelastic Properties of Polymers* 3rd edn (Wiley, 1980).
70. Li, J. et al. Thermorheological complexity of poly(vinyl alcohol)/borax aqueous solutions. *J. Rheol.* **64**, 991–1002 (2020).
71. Bischoff, D. J. et al. Unraveling the rheology of inverse vulcanized polymers. *Nat. Commun.* **14**, 7553 (2023).
72. Kannapadi, S. et al. The role of catalyst mobility and concentration on the linear viscoelasticity of associative dynamic covalent networks. *Macromolecules* **59**, 3465–3476 (2026).
73. Yount, W. C. et al. Small-molecule dynamics and mechanisms underlying the macroscopic mechanical properties of coordinatively cross-linked polymer networks. *J. Am. Chem. Soc.* **127**, 14488–14496 (2005).
74. Li, Y. et al. Dynamics of entangled metallosupramolecular polymer networks combining stickers with different lifetimes. *J. Rheol.* **66**, 1203–1220 (2022).
75. Zhuge, F. et al. Decoding the linear viscoelastic properties of model telechelic metallo-supramolecular polymers. *J. Rheol.* **61**, 1245–1262 (2017).
76. de Wergifosse, P. et al. Viscoelastic properties of metallo-supramolecular networks: relationship between sticker/entanglement dynamics and terminal relaxation. *Macromolecules* **58**, 222–239 (2025).
77. Wang, H. et al. Linear viscoelasticity of model vitrimers: decoding the interplay between bond exchange and segmental dynamics. *Macromolecules* https://doi.org/10.1021/acs.macromol.5c03092 (2026).
78. Huang, Q. et al. Stress growth and relaxation of dendritically branched macromolecules in shear and uniaxial extension. *J. Rheol.* **61**, 35–47 (2017).
79. McLeish, T. C. B. & Larson, R. G. Molecular constitutive equations for a class of branched polymers: the pom-pom polymer. *J. Rheol.* **42**, 81–110 (1998).
80. Bishko, G. et al. Theoretical molecular rheology of branched polymers: the pom-pom model. *Phys. Rev. Lett.* **79**, 2352 (1997).
81. Wang, S. et al. Contribution of unbroken strands to the fracture of polymer networks. *Macromolecules* **56**, 2309–2318 (2023).
82. Lentzakis, H. et al. Uniaxial extensional rheology of well-characterized comb polymers. *J. Rheol.* **57**, 605–625 (2013).
83. Lentzakis, H. et al. Pom-pom like constitutive equations for comb polymers. *J. Rheol.* **58**, 1855–1876 (2014).
84. Shabbir, A. Effect of hydrogen bonding on linear and nonlinear rheology of entangled polymer melts. *Macromolecules* **48**, 5988–5996 (2015).
85. Wang, W. Toward a design for flowable and extensible ionomers: an example of diamine-neutralized entangled poly(styrene-co-4-vinylbenzoic acid) ionomer melts. *Macromolecules* **53**, 2306–2315 (2021).
86. Wu, S. et al. Molecular design of highly stretchable ionomers. *Macromolecules* **51**, 4735–4746 (2018).
87. Arora, S. et al. Brittle fracture of polymer transient networks. *J. Rheol.* **61**, 1267–1275 (2017).
88. Ligoure, C. & Mora, S. Fractures in complex fluids: the case of transient networks. *Rheol. Acta* **52**, 91–114 (2013).
89. Yiming, B. et al. Elastic, strong and tough ionically conductive elastomers. *Nat. Commun.* **16**, 431 (2025).
90. Hoy, R. & Fredrickson, G. H. Thermoreversible associating polymer networks. I. Interplay of thermodynamics, chemical kinetics, and polymer physics. *J. Chem. Phys.* **131**, 224902 (2009).
91. Liu, S. et al. Brittle-to-ductile transition of sulfonated polystyrene ionomers. *ACS Macro Lett.* **10**, 503–509 (2018).
92. Slootman, J. et al. A molecular interpretation of the toughness of multiple network elastomers at high temperature. *Proc. Natl Acad. Sci. USA* **119**, e2116127119 (2022).
93. Song, Z. et al. Force-dependent bond dissociation explains the rate-dependent fracture of vitrimers. *Soft Matter* **17**, 6669–6674 (2021).
94. de Wergifosse, P. et al. Nonlinear shear and extensional rheology of telechelic metallosupramolecular networks. *Macromolecules* **59**, 4636–4649 (2026).
95. Pyromali, C. et al. Nonlinear shear rheology of single and double metal–ligand dynamic networks. *J. Rheol.* **66**, 1223–1235 (2022).
96. Inoue, T. et al. Nonlinear rheology of CTAB/NaSal aqueous solutions: finite extensibility of a network of wormlike micelles. *Langmuir* **21**, 1201–1208 (2005).
97. Vereroudakis, E. et al. Repeated shear startup response of a supramolecular polymer. *J. Nonnewton. Fluid Mech.* **315**, 105021 (2023).
98. Berret, J. F. & Séréro, Y. Evidence of shear-induced fluid fracture in telechelic polymer networks. *Phys. Rev. Lett.* **87**, 048303 (2001).
99. Ianniello, V. & Costanzo, S. Linear and nonlinear shear rheology of nearly unentangled H-polymer melts and solutions. *Rheol. Acta* **61**, 667–679 (2022).
100. Snijkers, F. et al. Start-up and relaxation of well-characterized comb polymers in simple shear. *J. Rheol.* **57**, 1079–1100 (2013).
101. Li, B. et al. Undershoot recovery in polystyrene melts: effects of annealing on repeated shear startup. *J. Phys. Chem. B* **130**, 533–546 (2025).

102. Coppola, S. et al. Rest-time effects in repeated shear-startup runs of branched SBR Polymers. *J. Rheol.* **58**, 1877–1901 (2014).
103. Snijkers, F. et al. Double stress overshoot in start-up of simple shear flow of entangled comb polymers. *ACS Macro Lett.* **2**, 601–604 (2013).
104. Gong, J. P. et al. Double network hydrogels with extremely high mechanical strength. *Adv. Mater.* **15**, 1155–1158 (2003).
105. Walker, S. B. & Fielding, S. M. Toughness of double network hydrogels: the role of reduced stress propagation. *Phys. Rev. Lett.* **135**, 188201 (2025).
106. Gong, J. P. Why are double network hydrogels so tough? *Soft Matter* **6**, 2583–2590 (2010).
107. Cui, K. & Gong, J. P. How double dynamics affects the large deformation and fracture behaviors of soft materials. *J. Rheol.* **66**, 1093–1111 (2022).
108. Yang, H. et al. Tunable interpenetrating polymer network hydrogels based on dynamic covalent bonds and metal–ligand bonds. *Macromolecules* **53**, 6956–6967 (2020).
109. Wang, F. S. Trapped entanglements in polymer networks. *Trends Chem.* **6**, 447–458 (2024).
110. Sun, T. L. et al. Physical hydrogels composed of polyampholytes demonstrate high toughness and viscoelasticity. *Nat. Mater.* **12**, 932 (2013).
111. Wei, Y. et al. Structural heterogeneity and its influence on nonlinear deformation and the fracture of ultrasoft hydrogels. *Macromolecules* **56**, 9604–9615 (2023).
112. Zheng, X. et al. Tuning the ultimate strain of single and double network gels through reactive strand extension. *ACS Cent. Sci.* **11**, 1882–1891 (2025).
113. Yang, H. et al. Influence of network topology on the viscoelastic properties of double dynamics hydrogels. *Macromolecules* **55**, 5058–5070 (2022).
114. Filippidi, E. et al. Toughening elastomers using mussel-inspired iron-catechol complexes. *Science* **358**, 502–505 (2017).
115. Yan, H. et al. How to choose a secondary interaction to improve stretchability of associative polymers? *Macromolecules* **54**, 8112–8121 (2021).
116. Mayumi, K. et al. Stress–strain relationship of highly stretchable dual cross-link gels: separability of strain and time effect. *ACS Macro Lett.* **2**, 1065–1068 (2013).
117. Narita, T. et al. Viscoelastic properties of poly(vinyl alcohol) hydrogels having permanent and transient cross-links studied by microrheology, classical rheometry, and dynamic light scattering. *Macromolecules* **46**, 4174–4183 (2013).
118. Ito, K. Novel cross-linking concept of polymer network: synthesis, structure, and properties of slide-ring gels with freely movable junctions. *Polym. J.* **39**, 489–499 (2007).
119. Kato, K. Dynamic transition between rubber and sliding states attributed to slidable cross-links. *Soft Matter* **7**, 8737–8740 (2011).
120. Ghiassinejad, S. et al. Effect of ring mobility on the dynamics of the slide-ring gels. *Chem. Mater.* **36**, 8311–8322 (2024).
121. Keith, A. N. et al. Bottlebrush bridge between soft gels and firm tissues. *ACS Cent. Sci.* **6**, 413–419 (2020).
122. Vatankhah-Varnosfaderani, M. et al. Chameleon-like elastomers with molecularly encoded strain-adaptive stiffening and coloration. *Science* **359**, 1509–1513 (2018).
123. Clarke, B. R. Bottlebrush networks: a primer for advanced architectures. *Angew. Chem. Int. Ed.* **63**, e202318220 (2024).
124. Scheutz, G. M. et al. Adaptable crosslinks in polymeric materials: resolving the intersection of thermoplastics and thermosets. *J. Am. Chem. Soc.* **141**, 16181–16196 (2019).
125. Montarnal, D. et al. Silica-like malleable materials from permanent organic networks. *Science* **334**, 965–968 (2011).
126. Van Zee, N. J. & Nicolaÿ, R. Vitrimers: permanently crosslinked polymers with dynamic network topology. *Prog. Polym. Sci.* **104**, 101233 (2020).
127. Röttger, M. et al. High-performance vitrimers from commodity thermoplastics through dioxaborolane metathesis. *Science* **356**, 62–65 (2017).
128. Zhang, B. et al. Recycling of vitrimer blends with tunable thermomechanical properties. *RSC Adv.* **9**, 5431–5437 (2019).
129. Clarke, R. W. et al. Dynamic crosslinking compatibilizes immiscible mixed plastics. *Nature* **616**, 731–739 (2023).
130. Tretbar, C. et al. Fluoride-catalyzed siloxane exchange as a robust dynamic chemistry for high-performance vitrimers. *Adv. Mater.* **35**, e2303280 (2023).
131. Castro, J. et al. Efficient and robust dynamic crosslinking for compatibilizing immiscible mixed plastics through in situ generated singlet nitrenes. *Adv. Mater.* **36**, e2406203 (2024).
132. Joosten, L. M. A. et al. Synthesis, recycling and high-throughput reprocessing of phase-separated vitrimer-thermoplastic blends. *Adv. Funct. Mater.* **34**, 2306882 (2024).
133. Torres, N. et al. Immiscible polydimethylsiloxane/polybutadiene vitrimer blends. *Macromolecules* **59**, 1330–1345 (2026).
134. Brunie, M.-I. et al. Phase-separated PVDF/vitrimer blends with enhanced mechanical and chemical stabilities obtained by reactive processing. *ACS Appl. Polym. Mater.* **8**, 1335–1345 (2026).
135. Ghosh, S. Impact of nanofillers on vitrimerization and recycling strategies: a review. *Nanoscale Adv.* **7**, 5842–5887 (2025).
136. Zhang, Z. et al. Recyclable vitrimer-based printed circuit boards for sustainable electronics. *Nat. Sustain.* **7**, 616–627 (2024).
137. Bates, F. S. & Fredrickson, G. H. Block copolymers — designer soft materials. *Phys. Today* https://doi.org/10.1063/1.882522 (1999).
138. Karayianni, M. & Pispas, S. Block copolymer solution self-assembly: recent advances, emerging trends, and applications. *J. Polym. Sci.* **59**, 1874–1898 (2021).
139. Akcora, P. et al. Anisotropic self-assembly of spherical polymer-grafted nanoparticles. *Nat. Mater.* **8**, 354–359 (2009).
140. Dhara, D. The payne effect in nanofilled cross-linked polyisoprene. *Macromolecules* **58**, 10559–10566 (2025).
141. van Steenberge, P. H. M. et al. Visualization and design of the functional group distribution during statistical copolymerization. *Nat. Commun.* **10**, 3641 (2019).
142. Gan, Z. et al. Precision polymers: advances in synthesis, structural engineering, and functional optimization. *Prog. Polym. Sci.* **170**, 102030 (2025).
143. Albertazzi, L. et al. Spatiotemporal control and superselectivity in supramolecular polymers using multivalency. *Proc. Natl Acad. Sci. USA* **110**, 12203–12208 (2013).
144. Feldman, K. E. et al. Model transient networks from strongly hydrogen-bonded polymers. *Macromolecules* **42**, 9072–9081 (2009).
145. Aida, T. & Meijer, E. W. Supramolecular polymers — we've come full circle. *Isr. J. Chem.* **60**, 33–47 (2020).
146. Likhtman, A. E. & McLeish, T. C. B. Quantitative theory for linear dynamics of linear entangled polymers. *Macromolecules* **35**, 6332–6343 (2002).
147. Baumgaertel, M. et al. The relaxation — time spectrum of nearly monodisperse polybutadiene melts. *Rheol. Acta* **31**, 75–82 (1992).
148. Shchetnikava et al. A comparison of tube model predictions of the linear viscoelastic behavior of symmetric star polymer melts. *Macromolecules* **47**, 3350–3361 (2014).
149. Hannecart, C. et al. Decoding the steady elongational viscosity of monodisperse linear polymers using tube-based modeling. *J. Rheol.* **66**, 197–218 (2022).
150. Costanzo, S. et al. Shear and extensional rheology of polystyrene melts and solutions with the same number of entanglements. *Macromolecules* **49**, 3925–3935 (2016).
151. Schußmann, M. G. Predicting maximum strain hardening factor in elongational flow of branched pom-pom polymers from polymer architecture. *Nat. Commun.* **15**, 3545 (2024).
152. Lyons, R. et al. Equilibration dynamics of a dynamic covalent network diluted in a metallosupramolecular polymer matrix. *J. Rheol.* **66**, 1349–1364 (2022).

Acknowledgements
This Review Article reflects a longtime collaboration of E.v.R. and D.V. and was written during exchange visits supported by the European Union's Horizon 2020 Programme for Research and Innovation under the Marie Skłodowska-Curie grant agreement no. 101119786 (ReBond). E.v.R. is Senior Research Associate of the FRS-FNRS.

Author contributions
Both authors contributed to all aspects of this work.

Competing interests
The authors declare no competing interests.

Additional information
Peer review information *Nature Reviews Physics* thanks Alexa Kuenstler and the other, anonymous, reviewer(s) for their contribution to the peer review of this work.

Publisher's note Springer Nature remains neutral with regard to jurisdictional claims in published maps and institutional affiliations.

Springer Nature or its licensor (e.g. a society or other partner) holds exclusive rights to this article under a publishing agreement with the author(s) or other rightsholder(s); author self-archiving of the accepted manuscript version of this article is solely governed by the terms of such publishing agreement and applicable law.

© Springer Nature Limited 2026